JOURNAL OF CATALYSIS 139, 576–590 (1993)

The Importance of Olefin Readsorption and H_2/CO Reactant Ratio for Hydrocarbon Chain Growth on Ruthenium Catalysts

ROSTAM J. MADON[1] AND ENRIQUE IGLESIA

Corporate Research Laboratories, Exxon Research and Engineering Co., Route 22 East, Annandale, New Jersey 08801

Received May 19, 1992; revised September 1, 1992

The synthesis of high molecular weight hydrocarbons on Ru catalysts requires the readsorption of primary α-olefin products. Such a readsorption step initiates a surface chain by reversing the β-hydrogen abstraction reactions: the chain termination step that forms an α-olefin. On Ru catalysts, 60 to 90% of $C_{21}+$ products require at least one readsorption event. These readsorption steps become increasingly important as chain size increases. This occurs because the diffusive removal of α-olefins from catalyst particles slows down significantly with increasing molecular size leading to long intraparticle residence times that favor secondary readsorption reactions. Chain growth probability and paraffin content therefore increase with molecular size. As a result, carbon number distributions do not obey simple Flory kinetics, an observation previously attributed to multiple chain growth sites and to the higher solubility of larger hydrocarbons in Fischer–Tropsch liquids. At low H_2/CO reactant ratios, where termination to olefins should be favored, large chains terminate only as paraffins. This again reflects the importance of diffusion-enhanced olefin readsorption which not only dominates bed residence time effects for large hydrocarbons but also weakens the effects of changes in reactant concentration. High H_2/CO reactant ratios lead to higher concentrations of hydrogen adatoms on Ru surfaces and thus favor chain termination to paraffins by hydrogen addition steps. Consequently, the contribution of olefin readsorption to chain growth and product molecular weight decreases markedly with increasing H_2/CO ratio.

INTRODUCTION

An important route to high value synthetic fuels requires the conversion of natural gas or coal to synthesis gas (CO and H_2), followed by the Fischer–Tropsch (FT) synthesis to high molecular weight aliphatic hydrocarbons and their ultimate upgrading to required products (*1*, *2*). Therefore the synthesis of high molecular weight hydrocarbons is commercially important. In Refs. (*3–7*), we described the critical role played by the readsorption of α-olefin products in hydrocarbon chain growth. Since Herington first suggested that this reaction occurs during FT synthesis (*8*), others, such as Pichler *et al.* (*9*, *10*), have discussed several secondary reactions, such as hydrogenation, hydrocracking, isomerization, and chain initiation that occur after α-olefins readsorb. Our recent work has identified catalyst properties and reaction conditions that favor α-olefin readsorption and chain initiation, and shown this reaction to be critical in the selective synthesis of heavy aliphatic hydrocarbons from CO and H_2.

The contribution of α-olefin readsorption reactions to chain growth increases as the residence time and the concentration (or more rigorously, the fugacity) of these reactive products increases within catalyst particles and reactors (*3–7*). Bed residence time and interparticle olefin concentrations increase with decreasing space velocity. Increased intraparticle (pore) residence time and olefin concentration gradients reflect diffusional restrictions that lower the rate of removal of reactive olefins from catalyst pores. Catalyst pores are filled with high

[1] Current address: Engelhard Corporation, 101 Wood Ave., Iselin, NJ 08830.

0021-9517/93 $5.00

molecular weight liquid hydrocarbon products during FT synthesis; therefore, intraparticle olefin diffusivity decreases markedly with increasing molecular size, consistent with reptation models of diffusion in polymer melts (*11*). Larger olefins remain longer within catalyst particles and are more likely to readsorb and initiate chains on FT synthesis sites (*3–7*).

Diffusion-enhanced readsorption of α-olefins leads to an increase in chain growth probability (α) with carbon number on Ru (*3–7*), Co (*5–7*), and Fe (*7*), until a constant asymptotic α value (α_a) is reached for large hydrocarbons. This accounts for the observed deviations of experimental carbon number distributions from Flory polymerization kinetics, where α is assumed to be independent of chain size. Such deviations lead to heavy hydrocarbon selectivities much greater than those predicted by Flory kinetics. High selectivity to heavy hydrocarbons is a feature of FT synthesis that strongly influences gas conversion process economics. In this study, we quantify the effectiveness of diffusion-enhanced olefin readsorption for hydrocarbon chain growth on Ru crystallites supported on TiO_2 and SiO_2. We also discuss how H_2/CO reactant ratios affect chain growth pathways and how molecular weight distributions are influenced by reactant composition and by olefin readsorption. Finally, we offer arguments to refute alternate explanations for the observed non-Flory distributions of FT products: the presence of two or more growth sites with different kinetics (*12*) and the longer reactor residence time of large hydrocarbons caused by their higher solubility in FT synthesis liquids (*13*).

EXPERIMENTAL

The experimental equipment and procedures have been described previously (*4*). Catalytic experiments were performed in a 1.22-m long, 0.77-cm internal diameter, stainless-steel fixed-bed reactor embedded in a copper block with a three-zone heater (*14*). Carbon monoxide, dihydrogen, carbon dioxide, and C_5- hydrocarbons were analyzed by on-line gas chromatography. Condensed C_5+ products, collected for about 24-h periods after reaching steady-state under each reaction condition, were analyzed using gas and high temperature gel-permeation chromatography.

Residence time experiments were performed by varying the H_2/CO flow rate at constant temperature, pressure, and reactant ratio (2.00 ± 0.03). The preparation, pretreatment, and characterization of 1.1% Ru/TiO_2 and 10.8% Ru/SiO_2 catalysts were reported elsewhere (*4*). Catalysts were prepared by contacting TiO_2 (Degussa P25) and SiO_2 (Davison, Grade 62) supports with a $Ru(NO_3)_3$ solution (Engelhard). The catalysts were reduced in flowing H_2 for 4 h at 723 K before catalytic experiments. Ru/TiO_2 was studied at 483 K, 550 kPa, and space velocities between 300 and 1500 V/V·h (86 to 17% CO conversion). Ru/SiO_2 was studied at 477 K, 550 kPa, and space velocities between 530 and 3000 V/V·h (81 to 14% CO conversion). Space velocity (GHSV) is defined here as the gas hourly reactant flow rate at STP per total bed volume. Reaction rates are almost independent of reactant conversion; they are reported as site-time yields, defined as the moles of CO converted per unit time per g-atom of surface Ru (*4*). For Ru/TiO_2 and Ru/SiO_2, the site-time yields are 2.2×10^{-2} and 1.8×10^{-2} s^{-1} respectively.

Reactant H_2/CO ratio effects on chain growth kinetics were studied on a 1.04% Ru/TiO_2 catalyst and on the 10.8% Ru/SiO_2 described above. This Ru/TiO_2 catalyst was prepared using the same procedure as the 1.1% Ru/TiO_2 sample used in residence time studies. This catalyst was studied at 488 K, 520 kPa, and H_2/CO reactant ratios of 1.02, 1.52, 2.0, and 2.8. The SiO_2-supported sample was studied at 490 K, 1515 kPa, and H_2/CO ratios of 2.0 and 3.23. When stoichiometric H_2/CO ratios (~2.0–2.1) are used, reactant ratios remain constant along the reactor bed and do not vary with CO conversion level or axial reactor position.

Reactant ratios above stoichiometric values lead to H_2/CO ratios that increase along the reactor as CO conversion increases. Conversely, values lower than the consumption stoichiometry lead to reactant ratios that decrease with increasing CO conversion. Except at very low CO conversions (<15%), reported rates, selectivities, and H_2/CO reactant ratios reflect average values along the catalyst bed.

Experimental results were not masked by catalyst deactivation, reactor temperature gradients, or intrapellet diffusional limitations of CO and H_2 (*4*).

RESULTS

Residence Time Effects

In previous reports, we have used carbon number-dependent chain termination (β_n) and growth (α_n) parameters to describe the FT product distributions on Ru (*3*, *4*) and Co (*5*, *6*) catalysts. The chain termination parameter compares the rate at which a growing chain terminates and desorbs as a C_n hydrocarbon ($r_{t,n}$) to the rate at which it continues to grow in the chain propagation step ($r_{p,n}$) (*8*). For a chain with n carbons (C_n),

$$\beta_n = \frac{r_{t,n}}{r_{p,n}} = \frac{\phi_n}{\sum_{i=n+1}^{\infty} \phi_i}. \quad (1)$$

This expression is related to the chain growth or Flory parameter (α_n) by

$$\alpha_n = \frac{1}{1+\beta_n} = \frac{\sum_{i=n+1}^{\infty} \phi_i}{\sum_{i=n}^{\infty} \phi_i}. \quad (2)$$

In Eqs. (1) and (2), ϕ_i is the molar rate of formation of C_i species during chain growth.

When α_n is independent of chain size, Eq. (2) becomes

$$\alpha = \frac{\phi_{n+1}}{\phi_n}. \quad (3)$$

This chain growth parameter is defined by the well-known Flory equation (*15*), written in its logarithmic form

$$\ln\frac{S_n}{n} = \ln\left[\frac{(1-\alpha)^2}{\alpha}\right] + n \ln \alpha, \quad (4)$$

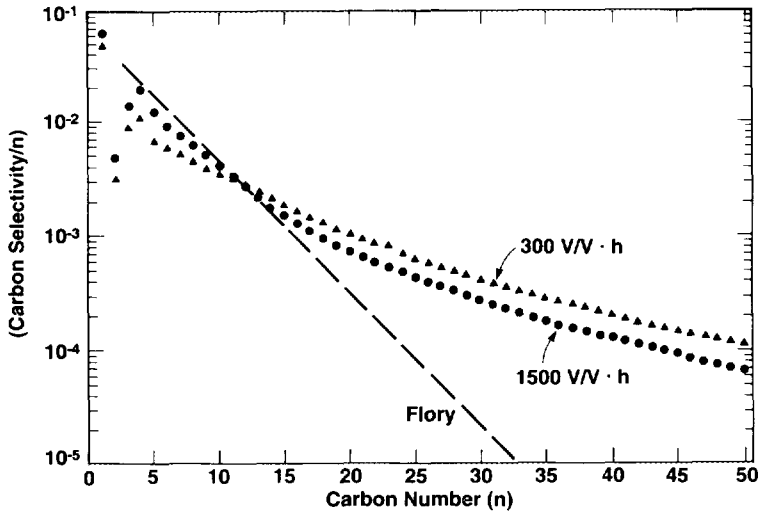

FIG. 1. Space velocity effects on FT synthesis carbon number distribution (1.1% Ru/TiO_2, 483 K, 550 kPa, $H_2/CO = 2.00 \pm 0.03$, 17 and 86% CO conversion).

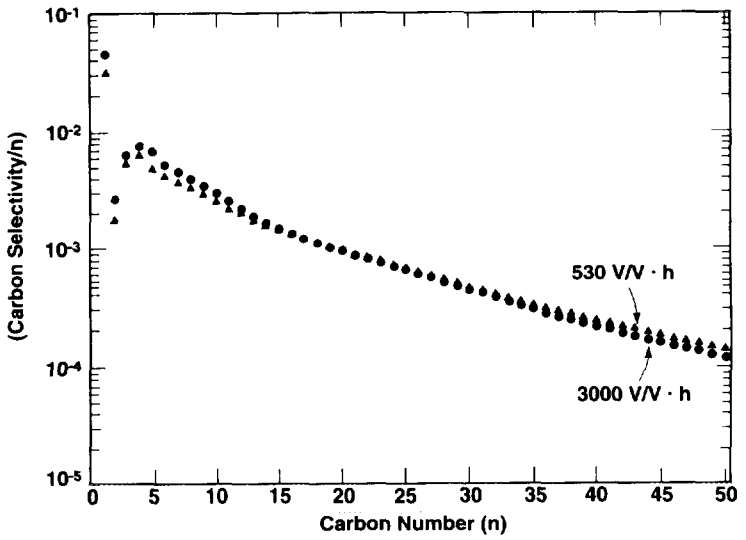

FIG. 2. Space velocity effects on FT synthesis carbon number distribution (10.8% Ru/SiO_2, 477 K, 550 kPa, $H_2/CO = 2.00 \pm 0.03$, 14 and 81% CO conversion).

where S_n is the carbon selectivity to C_n products. If the chain growth probability is independent of chain size, a plot of $\ln S_n/n$ versus n becomes a straight line, and the resulting distribution is fully described by a single value of α or β.

Product distributions on Ru/TiO_2 and Ru/SiO_2 catalysts are plotted in Figs. 1 and 2, respectively, using the form suggested by Eq. (4). Data at the highest and lowest space velocities are shown. In all cases, product distribution plots are initially curved but become linear for $C_{35}+$ hydrocarbons. In Fig. 1, the two space velocity plots intersect at about C_{12} and ultimately become parallel for $C_{35}+$ products. These data show that chain growth parameters initially increase with carbon number but become constant for $C_{35}+$ hydrocarbons. For smaller chains, α increases with decreasing space velocity and increasing conversion. This conversion dependence disappears above C_{35}, where the same α value of 0.932 describes the experimental data at both space velocities. The corresponding chain termination parameters (β_n) decrease with increasing carbon number and decreasing space velocity for chains smaller than C_{35}; β_n approaches a constant value of 0.0725, independent of space velocity or carbon number for larger chains (*4*). Chain termination to CH_4 (β_1) is also independent of space velocity (*3*, *4*), but β_4 increases as space velocity increases and approaches a value of 0.31 as bed residence time approaches zero (*4*). Therefore α_4 at very short bed residence time approaches 0.763 and is much lower than the 0.932 value of α_a for $C_{35}+$ hydrocarbons.

The same trends are observed on Ru/SiO_2 at slightly lower reaction temperatures (Fig. 2). Here, product distributions at high and low space velocities differ less than on Ru/TiO_2. Carbon number distributions do not follow conventional Flory kinetics and reach an asymptotic α_a value of 0.948 for $C_{35}+$ hydrocarbons that is independent of space velocity and CO conversion.

The paraffin content in C_2–C_{20} products increases with increasing carbon number and bed residence time (inverse space velocity) on Ru/TiO_2 (Fig. 3). Olefins are not ob-

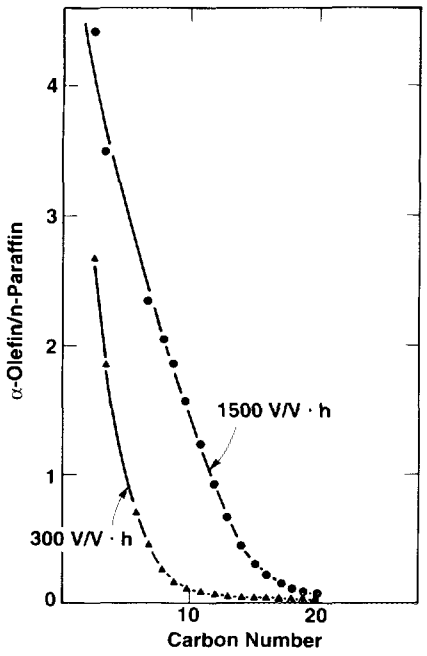

FIG. 3. Carbon number and space velocity effects on α-olefin/*n*-paraffin ratio (1.1% Ru/TiO2, 483 K, 550 kPa, H_2/CO = 2.00 ± 0.03, 17 and 86% CO conversion).

served in $C_{35}+$ products because their long pore residence time ensures that olefins will readsorb many times and initiate chains; only chains that terminate as unreactive paraffins exit the catalyst. Thus the higher paraffinic content of larger hydrocarbons is not the result of direct secondary hydrogenation of α-olefins to the corresponding paraffin of equal size (*3–7*), but reflects instead the enhanced readsorption of α-olefins and surface chain initiation steps that lead to the ultimate desorption of these α-olefins as larger products.

Individual termination parameters for olefins ($\beta_{n,o}$) and paraffins ($\beta_{n,h}$) versus carbon number at 300 and 1500 V/V·h (Fig. 4) confirm this proposal. In both cases, chain termination to olefins ($\beta_{n,o}$) decreases rapidly to zero, but termination to paraffins ($\beta_{n,h}$) increases only slightly and then remains constant. The large variation in $\beta_{4,o}$ with bed residence time is not caused by changes in the corresponding $\beta_{4,h}$ values, which are unaffected by conversion. This confirms our conclusion that the observed decrease in olefin selectivity is not caused by their secondary hydrogenation to the corresponding paraffin.

Reactant Composition Effects

The effects of H_2/CO ratio on FT synthesis rate and selectivity using Ru supported on TiO_2 and SiO_2 are shown in Tables 1 and 2, respectively. On Ru/TiO_2, data were obtained at the same space velocity except at the highest reactant ratio where, for selectivity comparisons, it was increased to 900 V/V·h in order to maintain H_2 + CO conversion levels close to those obtained for H_2/CO ratios of 1.02. High CO conversions magnify the effect of changes in H_2/CO ratios in nonstoichiometric feeds by causing a net increase or decrease in reactant ratio as conversion increases along the catalyst bed. Low CO conversion levels maintain H_2/CO ratios near inlet values; higher conversions (>20%) require that we use average bed ratios in selectivity comparisons. Selectivity

TABLE 1

Fischer Tropsch Synthesis on Ru/TiO_2: Effect of H_2/CO Ratio on Rate and Selectivity[a]

Inlet H_2/CO	1.02	1.52	2.03	2.8
GHSV, V/V·h	500	500	500	900
Exit H_2/CO	0.68	0.98	1.9	3.9
H_2 + CO conv, %	44	60	77	51
Site-time yields[b] [10^2·mol CO/g-atom surface Ru·s]	1.8	2.3	3.0	3.5
Selectivity[c]				
CH_4	2.5	3.1	4.4	7.2
C_2–C_4	5.9	5.9	7.1	8.9
C_5–C_{20}	41	44	48	51
C_{21}–C_{50}	29	32	29	26
$C_{51}+$	20	13	9	5

[a] 1.04% Ru/TiO_2, 488 K, 520 kPa. TiO_2: 40 m^2g^{-1} BET surface area, 13.5-nm average pore radius.

[b] Average Ru particle diameter, 2.2 nm; 0.5 dispersion assuming hemispherical crystallites.

[c] Remaining products, CO_2 and water soluble alcohols.

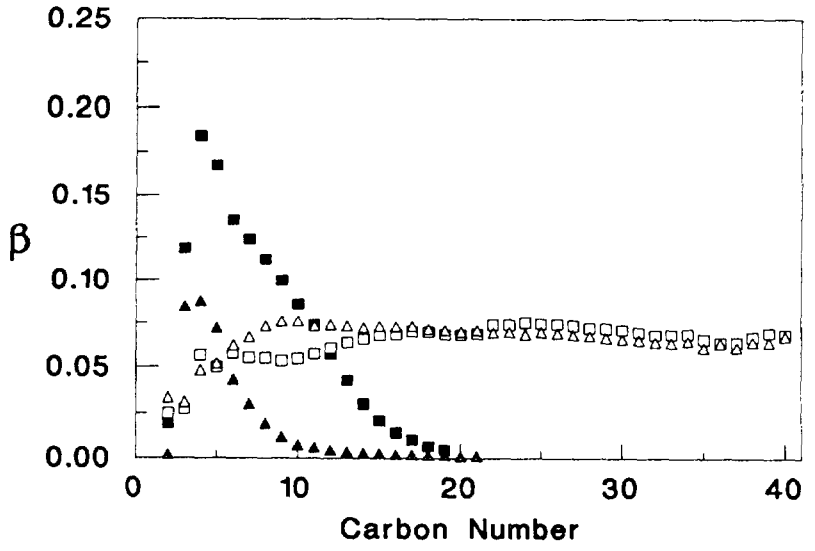

FIG. 4. Carbon number and space velocity effects on chain termination to α-olefins and n-paraffins (1.1% Ru/TiO_2, 483 K, 550 kPa, $H_2/CO = 2.00 \pm 0.03$) [1500 V/V·h, 17% conversion, olefins (■), paraffins (□); 300 V/V·h, 86% conversion, olefins (▲), paraffins (△)].

trends can be obtained even at the intermediate but similar conversion range of the data in Table 1. On Ru/TiO_2, site-time yields increase by a factor of 2 as inlet H_2/CO ratios increase from 1.02 to 2.8, consistent with the negative order CO kinetics previously reported on these Ru catalysts (*5*, *6*). The products become lighter as reactant ratios increase. Methane selectivity increases by about a factor of three and $C_{51}+$ yields decrease by a factor of five in this range of reactant composition.

Carbon number distribution plots are curved at all reactant concentrations on Ru/TiO_2 catalysts. Fig. 5 shows carbon number distributions at inlet H_2/CO ratios of 1.02 and 2.8; product molecular weight increases with decreasing H_2/CO ratios. This arises from the lower chain termination parameter (β_n) observed for all carbon numbers at lower reactant ratios (Fig. 6). Asymptotic values of the chain termination parameter are much lower at reactant ratios of 1.02 ($\beta_a = 0.044$) than at 2.8 ($\beta_a = 0.08$). Values of β_a increase monotonically with increasing H_2/CO ratio (Fig. 7a). The chain termination

TABLE 2

Fischer–Tropsch Synthesis on Ru/SiO_2: Effect of H_2/CO Ratio on Rate and Selectivity[a]

Inlet H_2/CO	2.02	3.2
GHSV, V/V·h	5150	7500
Exit H_2/CO	2.02	3.5
$H_2 + CO$ conv. %	20	15
Site-time yields[b] [10^2·mol CO/g-atom surface Ru·s]	4.3	5.7
Selectivity[c]		
CH_4	5.3	8.1
C_2–C_4	7.1	7.7
C_5–C_{20}	43	47
C_{21}–C_{50}	30	27
$C_{51}+$	9.5	5.2
β_1	0.62	0.88
β_a	0.067	0.081

[a] 10.8% Ru/SiO_2, 490 K, 1510 kPa. SiO_2: 280 m^2g^{-1} BET surface area, 6.5-nm average pore radius.

[b] 0.20 Dispersion by H_2 chemisorption.

[c] Remaining products, CO_2 and water soluble alcohols.

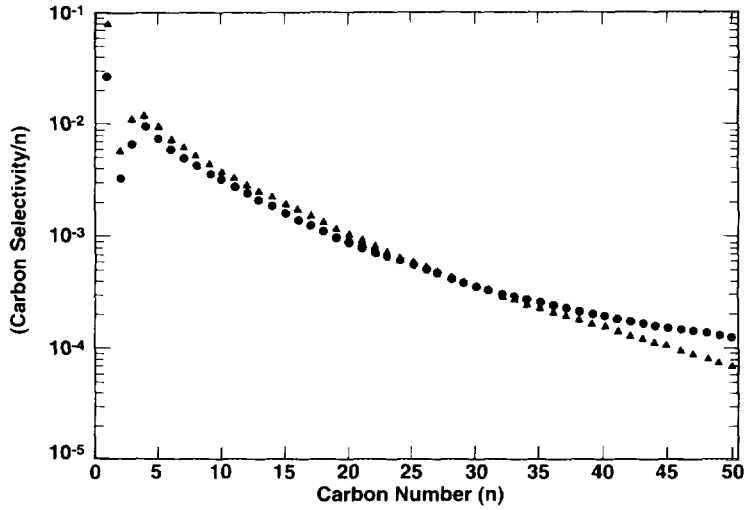

FIG. 5. The effect of reactant H_2/CO ratio on FT synthesis carbon number distribution [1.04% Ru/TiO_2, 488 K, 520 kPa; H_2/CO = 2.8, 51% (H_2 + CO) conversion (▲); H_2/CO = 1.02, 44% (H_2 + CO) conversion (●)].

parameter for methane (β_1), previously related to the rate of hydrogen addition to surface methyl species (*4–6*), also increases from 0.30 to 0.72 as reactant ratios increase from 1.02 to 2.8 on Ru/TiO_2 (Fig. 7b). Both β_a and β_1 reflect the availability of surface hydrogen for hydrogen addition termination steps, which increases with increasing H_2 concentration in the gas phase.

α-Olefin to *n*-paraffin ratios decrease with increasing carbon number at all reactant concentrations (Fig. 8). α-Olefins are not detected among C_{25}+ hydrocarbons, even at the lowest exit ratios (H_2/CO = 0.68), conditions that normally favor olefins and which selectively inhibit chain termination to paraffins; indeed, products are predominantly paraffinic in the C_{25}+ range at both low (0.68) and high exit ratios (3.9).

Chain termination parameters for α-olefins ($\beta_{n,o}$) and *n*-paraffins ($\beta_{n,h}$) show similar trends at 1.02 and 2.8 H_2/CO ratios (Fig. 9). Chain termination to α-olefins decreases with increasing chain size; β_o decreases from 0.11 for 1-butene to 0 for C_{25}+ hydrocarbons at low H_2/CO ratios (1.02) and from 0.096 to 0 at higher ratios (2.8). Apparently a higher selectivity for chain termination to olefins at low H_2/CO ratios is balanced by a similarly higher readsorption rate, consistent with the first-order dependence of olefin readsorption rates. In contrast, chain termination to paraffins increases with increasing H_2/CO ratio; β_h increases from 0.025 for *n*-butane to an asymptotic value of 0.044 at 1.02 H_2/CO ratio, and similarly from 0.051 to 0.0818 at the higher ratio of 2.8. Chain termination to paraffins is clearly favored at high H_2/CO ratios. Paraffins and internal olefins account for all termination products of C_{25}+ chains because termination pathways to α-olefins are totally reversed by readsorption. Lighter products are obtained at higher H_2/CO reactant ratios that favor intrinsic termination of surface chains as paraffins; this termination step cannot be reversed in subsequent secondary reactions because of thermodynamic constraints on the rate of the reverse reaction.

Similar trends are observed on Ru/SiO_2 catalysts (Table 2). These data were obtained at lower CO conversion levels than

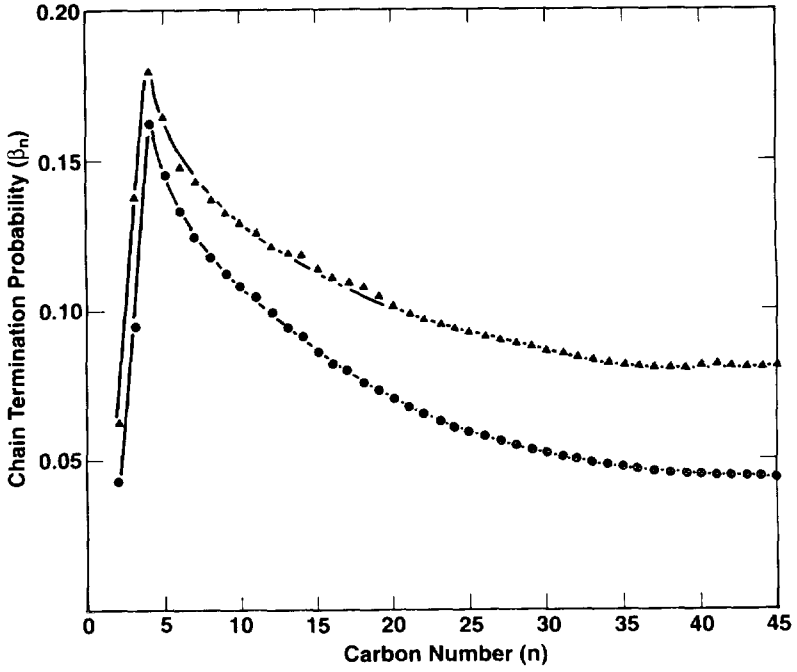

FIG. 6. Reactant composition and carbon number effects on chain termination probability [1.04% Ru/TiO_2, 488 K, 520 kPa; H_2/CO = 2.8, 51% (H_2 + CO) conversion (▲); H_2/CO = 1.02, 44% (H_2 + CO) conversion (●)].

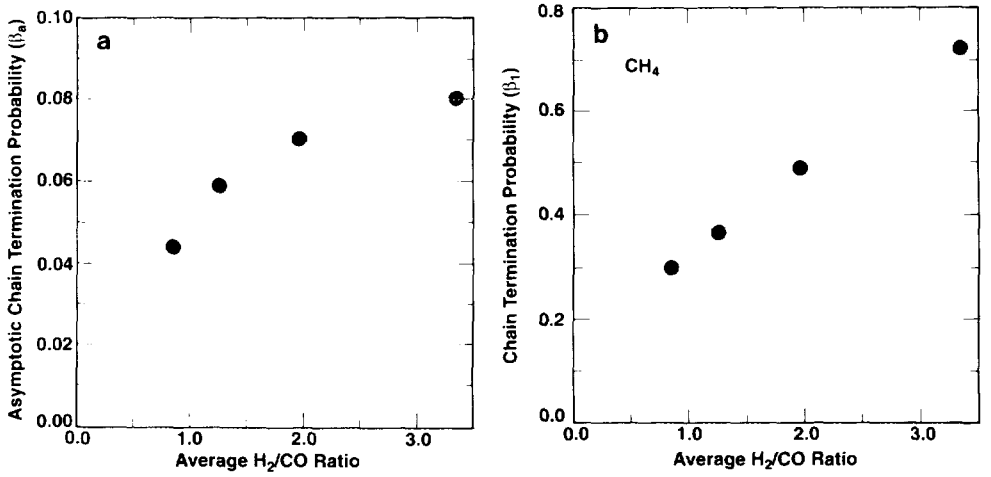

FIG. 7. Reactant composition effects on chain termination probability. (a) Asymptotic chain termination probability (β_a, $C_{35}+$); (b) methane chain termination probability (β_1). 1.04% Ru/TiO_2, 488 K, 520 kPa.

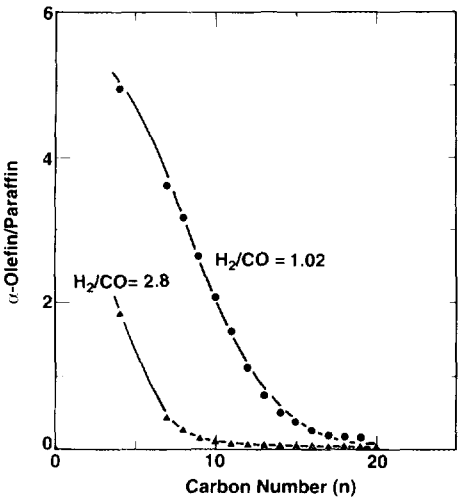

FIG. 8. Reactant composition and carbon number effects on α-olefin/*n*-paraffin ratio [1.04% Ru/TiO_2, 488 K, 520 kPa; H_2/CO = 2.8, 51% (H_2 + CO) conversion (▲); H_2/CO = 1.02, 44% (H_2 + CO) conversion (●)].

on TiO_2-supported catalysts. Therefore reactant concentration gradients along the catalyst bed are much weaker. Changes in product selectivity with increasing reactant ratio are very similar to those reported in Table 1 for Ru/TiO_2 catalysts even though experimental conditions differ. Methane (β_1) and asymptotic (β_a) chain termination parameters also follow trends similar to those on Ru/TiO_2. Chain termination parameters for all carbon numbers are smaller at the lower H_2/CO ratio. Consequently chain growth parameters and product molecular weight increase with decreasing reactant ratio, primarily because of the selective inhibition of hydrogen addition termination steps.

DISCUSSION

Residence Time Effects

The *diffusion-enhanced olefin readsorption model*, mentioned briefly in the Introduction and previously discussed in detail (*3–7*), provides a simple explanation for the trends in Figs. 1–4. Selectivity and β values for light hydrocarbons increase with increasing space velocity because α-olefins are removed more rapidly from the catalyst bed; thus their interparticle concentration and bed residence time decrease, leading to lower rates of secondary readsorption reac-

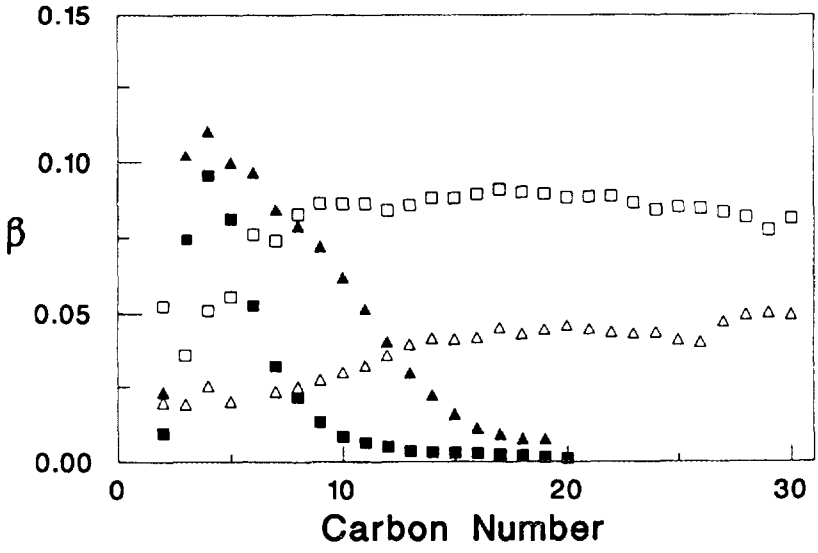

FIG. 9. Reactant composition and carbon number effects on chain termination to α-olefins and *n*-paraffins (1.04% Ru/TiO_2, 488 K, 520 kPa) [H_2/CO = 2.80, 51% conversion, olefins (■), paraffins (□); H_2/CO = 1.02, 44% conversion, olefins (▲), paraffins (△)].

tions. This bed residence time effect resembles the intraparticle residence time effect that leads to the observed effects of carbon number on olefin content and chain termination probability (Figs. 1–4). Increasing the residence time of reactive α-olefins within the catalyst bed (by slow convection) and within catalyst particles (by slow diffusion) leads to the selective inhibition of chain termination to olefins as bed residence time and carbon number increase (Figs. 3 and 4).

As carbon number increases, reactive α-olefins become increasingly difficult to remove from liquid-filled catalyst pores, and intraparticle diffusion becomes the dominant transport mechanism controlling residence time and readsorption probability. Chain termination probabilities become independent of space velocity and carbon number when intraparticle residence times become so large that no olefins exit the catalyst particles and only paraffins remain as stable termination products. This occurs on Ru catalysts, under our experimental conditions, for $C_{35}+$ hydrocarbons.

Without diffusion-enhanced olefin readsorption, FT synthesis on Ru would lead to much lighter products. In order to estimate what fraction of the heavy hydrocarbons requires α-olefin readsorption and chain initiation, we compare observed product distributions with those predicted from conventional Flory kinetics, i.e., without α-olefin readsorption. On Ru/TiO_2, β_4 data extrapolated to infinite space velocity gives an intrinsic chain termination value of 0.31 (*4*), which corresponds to an α_4 value of 0.763. If the intraparticle residence time of a small molecule, such as 1-butene, is sufficiently short to prevent readsorption, its intrinsic chain growth parameter also describes the entire distribution ($\alpha = 0.763$, smaller if 1-butene readsorption actually occurred). The Flory plot generated by this chain growth parameter is shown as a dashed line in Fig. 1. Below we compare the product selectivities predicted by these readsorption-free chain growth processes with those obtained experimentally on Ru catalysts.

Flory kinetics on Ru/TiO_2 ($\alpha = 0.763$) would lead to 2.6 wt% $C_{21}+$ selectivity and only 0.02 wt% $C_{41}+$ selectivity. Experimental values at 300 V/V·h on Ru/TiO_2 are 39.6 and 14.5 wt% for $C_{21}+$ and $C_{41}+$ respectively. Thus, 93% of $C_{21}+$ chains and 99.8% of $C_{41}+$ chains require at least one α-olefin readsorption event. These desirable readsorption events require that α-olefins be reactive and that their pore and bed residence time be increased significantly by transport restrictions.

The relative importance of pore (intraparticle) and bed residence time effects can be compared by noting that the data at 1500 V/V·h predominantly reflect pore residence time effects, because olefins leave the catalyst bed sufficiently fast to prevent readsorption within particles below. Therefore the difference between the curves at 300 and 1500 V/V·h in Fig. 1 reflects bed residence time effects on secondary readsorption reactions. In contrast, the difference between the curve at 1500 V/V·h and the dashed Flory line reflects the true effect of intraparticle diffusion on α-olefin readsorption. At 1500 V/V·h, $C_{21}+$ selectivity is 28.4 wt% and $C_{41}+$ selectivity is 10.3 wt%, compared with values of 39.6 and 14.5 wt% at 300 V/V·h. Even at high space velocity, 91% of $C_{21}+$ chains and 99.8% of $C_{41}+$ require at least one readsorption event; these chains form only because diffusion-limited readsorption of olefins within catalyst particles effectively reverses the predominant β-hydrogen abstraction chain termination pathway. At 300 V/V·h, of the $C_{21}+$ products resulting from α-olefin readsorption, 30% arise from bed residence time effects and 70% from intraparticle diffusion effects. For $C_{41}+$ products, the corresponding values are 29 and 71%.

FT synthesis products are heavier on Ru/SiO_2 than on Ru/TiO_2, predominantly because of the lower reaction temperature. Space-velocity effects on product distribution are weaker than on Ru/TiO_2 (Fig. 2).

The marked curvature in carbon number distribution plots and the small selectivity differences between high and low bed residence times suggest that readsorption occurs predominantly within diffusion-limited particles on this Ru/SiO_2 catalyst. Even light products are affected by diffusion-enhanced readsorption on Ru/SiO_2 particles; therefore, the β_4 value obtained at high space velocity is already lower than the intrinsic (readsorption-free) value. Yet we will use it as a lower limit to the intrinsic value of the Flory chain termination parameter. This value of β_4 is 0.149 and leads to an α_4 value of 0.87.

This value of α_4, applied to the entire carbon number distribution (i.e., Flory kinetics), predicts $C_{21}+$ and $C_{41}+$ carbon selectivities of 22.0 and 2.4 wt%, respectively; the corresponding experimental values at 530 V/V·h are 53.6 and 26.4 wt%. Even though we have overestimated the intrinsic α value, 60% of the $C_{21}+$ and 91% of the $C_{41}+$ products require olefin readsorption events; they would not form in a single surface sojourn using intrinsic chain growth pathways. For $C_{21}+$ products requiring at least one α-olefin readsorption event, 16% arise from bed residence time effects and 84% from pore residence time effects at 530 v/v·h. For $C_{41}+$ products, the corresponding values are 15 and 85%. The greater contribution of intraparticle readsorption on Ru/SiO_2 reflects both a higher intrinsic readsorption probability at lower reaction temperatures and the more severe intraparticle diffusional resistances caused by the higher volumetric density of chain growth (and readsorption) sites on the SiO_2-supported catalyst.

The relative importance of pore and bed residence times at a given conversion is independent of chain size for $C_{21}+$ products. This is consistent with our proposal that bed residence time effects arise from the readsorption of smaller α-olefins; these effects become negligibly small for large $C_{21}+$ α-olefins that react predominantly within the catalyst particle and seldom leave these particles unreacted. As they move along the catalyst bed by forced convection, small olefins diffuse into catalyst particles and initiate surface chains that continue to grow and ultimately desorb as higher hydrocarbons. The effectiveness of convective removal increases with increasing space velocity. Therefore space velocity affects $C_{21}+$ selectivity only indirectly by reintroducing lighter chains into chain growth pathways and thus changing the surface density of $C_{21}+$ growing chains. This gives rise to the space velocity effects on selectivity shown in Figs. 1 and 2, even for chain lengths for which chain growth parameters become independent of chain size. As olefins become larger, they are less likely to leave a pellet unreacted, and when they do, they are also less likely to diffuse into other catalyst particles because of intraparticle diffusion limitations.

Our selectivity estimates assume that diffusional restrictions do not affect 1-butene readsorption because short hydrocarbon chains diffuse rapidly within intrapellet liquids. If 1-butene readsorbs, then estimated α values on Ru/SiO_2 (0.87) and on Ru/TiO_2 (0.763) become upper limits. Consequently the actual contribution of diffusion-enhanced olefin readsorption to heavy hydrocarbon synthesis would be even greater than our estimates suggest. Our results show that diffusion-enhanced olefin readsorption accounts not only for the non-Flory carbon number distributions but also for the high paraffin wax selectivity obtained by FT synthesis on Ru catalysts. Intrinsic chain growth (Flory) kinetics are unable to provide such high yields of heavy hydrocarbons without significant olefin readsorption and strong enhancements of these reactions by intraparticle diffusional restrictions.

Reactant Composition Effects

Chain termination parameters (β_n) increase with increasing H_2/CO reactant ratio for all carbon numbers (Fig. 5). The overall chain termination parameter can be ex-

pressed as a linear combination of values for individual termination steps (*3*),

$$\beta_n = r_{t,n}/r_p = (r_h + r_o + r_i - r_{r,n})/r_p$$
$$= \beta_h + \beta_o + \beta_i - \beta_{r,n}, \quad (5)$$

where the subscripts h, o, and i refer to chain termination as paraffins, α-olefins, and isomers. The latter, predominantly 2-olefins and branched paraffins, are minor components in the products; they are also much less reactive than α-olefins (*4*). The subscript r refers to a readsorption step, the reverse of the H-abstraction step that leads to termination as α-olefins and the only reaction step in our model with kinetics that depend on chain size. For large n, r_r approaches the value of r_o; then, β_o equals β_r, and the net rate of olefin formation approaches zero (*3*, *4*). Consequently chain termination as paraffins becomes the predominant termination step, and β_h approaches the asymptotic chain termination parameter (β_a),

$$\beta_{a,\nu} = \beta_{h,\nu} = (k_h/k_p) \cdot \rho_\nu, \quad (6)$$

where the subscript ν denotes the reactant ratio (H_2/CO). The parameter ρ is the ratio of the concentration of adsorbed hydrogen (H*) and chain growth surface intermediates (*CH_2):

$$\rho = (H^*)/(^*CH_2). \quad (7)$$

Equations (6) and (7) reflect law of mass action kinetics for the rates of chain termination,

$$^*C_nH_{2n+1} + H^* \rightleftarrows C_nH_{2n+2} + 2^*, \quad (8)$$

and propagation,

$$^*C_nH_{2n+1} + {}^*CH_2 \rightleftarrows {}^*C_{n+1}H_{2n+3} + {}^*. \quad (9)$$

If we assume that intrinsic propagation and termination rate constants are independent of reactant composition, the ratio of asymptotic termination parameters at two reactant ratios becomes

$$\beta_{a,\nu'}/\beta_{a,\nu''} = \rho_{\nu'}/\rho_{\nu''}. \quad (10)$$

On Ru/TiO_2, this ratio equals 1.8 for reactant ratios of 2.8 and 1.02. Therefore, (H*)/(*CH_2) ratios are 1.8 times greater at the higher H_2/CO ratio.

From the law of mass action kinetics for chain termination to paraffins [Eq. (8)] and olefins,

$$^*C_nH_{2n+1} \rightleftarrows C_nH_{2n} + H^*, \quad (11)$$

we obtain the ratio of these two termination parameters:

$$\beta_h/\beta_o = \rho_h/\rho_o = (k_h/k_o)(H^*). \quad (12)$$

Thus the concentration of surface hydrogen (H*) determines chain termination probabilities and olefin content on Ru. This value of β_h/β_o increases with increasing H_2/CO ratio on all Ru catalysts studied. Fewer olefins are formed at higher reactant ratios, the contribution of olefin readsorption to chain growth decreases, and β_h increases with increasing hydrogen content in the feed. Therefore $\beta_{n,2.8}$ is greater than $\beta_{n,1.05}$ for all values on n. However, the curved Flory plots (Fig. 5) and the decreasing β_n values with increasing chain size (Fig. 6) show that olefin readsorption remains an important chain initiation process, and strongly influences carbon number distribution and olefin/paraffin selectivity at all reactant compositions used in our study.

Low hydrogen concentrations in the feed favor low surface hydrogen concentrations and termination of surface chains as olefins instead of paraffins. Low H_2/CO ratios lead to higher olefin to paraffin ratios for small hydrocarbons (Fig. 8). Larger hydrocarbons, however, terminate only as paraffins, regardless of reactant ratio because of diffusional restrictions. Olefin fugacity gradients within catalyst pores are undoubtedly affected by changes in reactant composition, but in all cases, olefin fugacities at the outer particle surfaces become negligible for large olefins. Thus diffusion-enhanced olefin readsorption not only reverses olefin termination steps and removes bed residence time effects for large molecules, but also weakens the effects of changes in reactant concentration, which in the absence of diffu-

sional effects, control termination probabilities to olefins and paraffins.

Non-Flory Distributions in Fischer–Tropsch Synthesis

Pichler and co-workers (*10*) first reported that chain growth probabilities on Co catalysts increased with chain size in the C_{10}–C_{16} range; they suggested that a higher rate of readsorption for larger olefins accounts for this behavior. Schulz *et al.* (*16*) noted that the phase in which products leave the reactor shifted from the gas to the liquid phase in this hydrocarbon size range. They proposed that the predominant removal of large hydrocarbons in the liquid phase leads to much longer residence times. Later, Schulz and co-workers (*13*) suggested that this higher residence time reflects the greater solubility of larger hydrocarbons in Fischer–Tropsch liquids. We have shown, however, that the presence of a liquid phase within catalyst pores affects selectivity only when it introduces a transport barrier to either product removal or reactant arrival (*3, 5*). A liquid phase must perturb the concentration (fugacity) of a chemical species in solution from the value it reaches when equilibrated with a contacting gas phase in order to affect the rate and selectivity of any chemical reaction.

In the absence of intraparticle diffusional limitations, products are present at equilibrium concentrations within liquid-filled pores, and gas (g) and liquid (l) phase fugacities (f) are identical for each component. When standard states are chosen for both phases, fugacities become equivalent to thermodynamic activities; they are related to concentrations by γ, the activity coefficient. At equilibrium,

$$f_g = f_l = \gamma_g C_g = \gamma_l C_l. \qquad (13)$$

Chemical reaction rates are directly proportional to the concentration of the transition state (†) (*17*) and given by

$$r = (kT/h)C^{\dagger}, \qquad (14)$$

where the universal constant (kT/h) is approximately 10^{13} s^{-1}. Also, transition states are assumed to be in equilibrium with reactants, and their fugacities are related by the equilibrium constant

$$K^{\dagger} = f^{\dagger}/f_{i,l}. \qquad (15)$$

Combining these equations leads to

$$r = (kT/h)(K^{\dagger}/\gamma^{\dagger})(\gamma_{i,l}C_{i,l}) = (kT/h)(K^{\dagger}/\gamma^{\dagger})(\gamma_{i,g}C_{i,g}). \qquad (16)$$

This equation clearly shows that when gas and liquid phase fugacities are identical (i.e., in the absence of transport restrictions), the presence of a liquid phase does not enter the kinetic treatment of chemical reaction rates. Specifically, at vapor–liquid equilibrium conditions, the higher relative concentrations (solubility) of larger α-olefins in hydrocarbon liquids cannot increase the rate of their secondary readsorption and chain initiation reactions. The rate of such readsorption reactions is determined by the α-olefin fugacity, which remains equal to its gas phase value for all hydrocarbons, irrespective of the presence of a liquid phase within catalyst pores. Without transport restrictions, changes in space velocity would affect olefin residence times and concentrations both inside and outside catalyst particles to the same extent. Also, the rate of convective removal of reactive olefins is identical for all hydrocarbons, irrespective of size; thus, convective removal processes cannot give rise to the observed effects of carbon number selectivity. In effect, the presence of an inert liquid phase is detected by a chemical reaction only when it introduces a transport restriction. When it does not, the presence of a liquid cannot lead to the observed carbon number effects on chain termination probability and olefin content.

Deviations from conventional Flory plots were also previously attributed to the presence of two or more types of chain growth sites with different chain growth kinetics (*12*), a proposal later used by many others to explain their results (*18–21*). Many reports of non-Flory distributions undoubtedly reflect artifacts resulting from selectiv-

ity data in limited carbon number ranges or from inadequate mass balances and product collection procedures. Other reports clearly reflect ineffective dispersal of promoters and site heterogeneity introduced during catalyst synthesis. Yet, the remaining examples reflect readsorption probabilities influenced by the different diffusivities of hydrocarbon chains of varying size.

The dual or multiple-site model of non-Flory distributions cannot explain the following results reported here for Ru and elsewhere on Ru (*3*, *4*, *7*), Co (*5–7*), and Fe (*7*) catalysts. For example,

(i) α increases (β decreases) monotonically with increasing bed residence time and carbon number in the C_2 to C_{35} molecular size range, but becomes independent of both for $C_{35}+$ hydrocarbons.

(ii) α-Olefin/n-paraffin ratios decrease rapidly with increasing carbon number and bed residence time, irrespective of reactant composition or surface H and CO concentrations; olefin contents in smaller chains increase as bed residence time or H_2/CO ratio decreases but larger hydrocarbons are exclusively paraffinic irrespective of bed residence time, carbon number, or H_2/CO ratio.

(iii) Only the olefin component of the chain termination parameter decreases with increasing chain size and bed residence time; the paraffin component is almost unaffected and actually increases slightly with increasing chain length (Fig. 4); this remains true at high space velocities (low conversions) where bed residence times become negligible.

(iv) Readsorption efficiency and C_5+ selectivity increase as transport restrictions become more severe with increasing Ru or Co site density or with increasing catalyst particle size (*3–6*).

(v) Theoretical diffusion-enhanced readsorption models are in quantitative agreement with experimental results on both Co and Ru catalysts (*3–6*), as expected from their similar chain growth and readsorption kinetics; this kinetic resemblance between Co and Ru catalysts is unlikely to arise from similar dual-site behavior in two catalytic elements of quite different reducibility and crystallite size.

(vi) Carbon number and bed residence time have similar effects on chain growth and olefin selectivity, suggesting that they reflect secondary reactions enhanced by transport restrictions (diffusive or convective).

(vii) Small and large hydrocarbons are influenced differently by transport restrictions, not only in olefin and paraffin content as described in (ii) but in the way that *cis*-2-olefin/*trans*-2-olefin ratios approach equilibrium as carbon number and bed residence time increase (*3*, *4*).

Clearly, diffusion-enhanced readsorption of α-olefins accounts in a simple manner for many of the common features of chain growth on Ru, Co, and Fe catalysts: the non-Flory distribution of hydrocarbons, the rapid decrease in olefin content with increasing hydrocarbon size, the increase in product molecular weight as transport restrictions become more severe with increasing pellet size or readsorption site density, and the high selectivity to paraffinic wax, not expected from chain growth kinetics measured for small chains. This model collapses to the simple Flory kinetic model when secondary hydrogenation reactions or conditions leading to preferential termination of surface chains as paraffins preclude extensive readsorption and chain initiation by α-olefins during FT synthesis (*7*). It appears unnecessary to propose different types of sites in order to explain the preferential formation of paraffins at high carbon numbers (*20*), or to propose changes in intrinsic surface chain growth pathways and reactive intermediates with increasing chain size (*22*) in order to explain observed deviations from Flory kinetics. Our *diffusion-enhanced α-olefin readsorption* model for chain growth effectively replaces multi-site and enhanced solubility models of non-Flory product distributions with a much simpler proposal that is consistent with

available experimental results on Ru, Co, and Fe catalysts.

CONCLUSIONS

Intrinsic chain growth pathways are insufficient to produce the high wax yields observed on Ru catalysts without significant readsorption of α-olefins; a secondary reaction enhanced by diffusional restrictions that prevent the rapid removal of these reactive molecules from liquid-filled catalyst pellets. A major fraction of the $C_{21}+$ products would not form without diffusion-enhanced olefin readsorption pathways. These pathways account for the non-Flory distribution of hydrocarbons, and for the increase in chain growth probability and paraffin content as carbon number and bed residence time increase. This proposal replaces previous explanations that invoke multiple chain growth sites and solubility arguments, neither of which account for many of the selectivity features observed in Fischer–Tropsch synthesis.

Intrinsic chain growth kinetics depend on reactant H_2/CO ratio. Chain termination to paraffins by hydrogen addition to alkyl groups is favored by high hydrogen adatom concentrations at high H_2/CO ratios. In contrast with hydrogen abstraction steps leading to olefins, which are reversed by olefin readsorption and chain initiation reactions, chain termination to paraffins is irreversible under Fischer–Tropsch synthesis conditions. Thus as H_2/CO ratio increases, the contribution of olefin readsorption to chain growth decreases, chain termination rates increase, and this results in a lighter more paraffinic product.

REFERENCES

1. Dry, M. E., *in* "Catalysis–Science and Technology" (J. R. Anderson and M. Boudart, Eds.), Vol. 1, p. 231. Springer-Verlag, Berlin, 1981.
2. Eilers, J., Posthuma, S. A., and Sie, S. T., *Catal. Lett.* **7,** 253 (1990).
3. Iglesia, E., Reyes, S. C., and Madon, R. J., *J. Catal.* **129,** 238 (1991).
4. Madon, R. J., Reyes, S. C., and Iglesia, E., *J. Phys. Chem.* **95,** 7795 (1991).
5. Iglesia, E., Reyes, S. C., and Soled, S. L., *in* "Computer-Aided Design of Catalysts and Reactors" (Pereira, C. J., and Becker, R. E., Eds.), Dekker, New York, in press.
6. Iglesia, E., Reyes, S. C., Madon, R. J., and Soled, S. L., *in* "Advances in Catalysis and Related Subjects" (Pines, H., Eley, D. D., and Weisz, P. B., Eds.), Vol. 38. Academic Press, New York, 1992.
7. Madon, R. J., Iglesia, E., and Reyes, S. C., *in* "Selectivity in Catalysis," ACS Symposium Series (Suib, S. L., and Davis, M. E., Eds.), in press.
8. Herington, E. F. G., *Chem. Ind.* **347** (1946).
9. Pichler, H., Schulz, H., and Elstner, M., *Brenst. Chem.* **48,** 78 (1967).
10. Pichler, H., Schulz, H., and Hojabri, F., *Brenst. Chem.* **45,** 215 (1964).
11. DeGennes, P., *J. Chem. Phys.* **55,** 572 (1971).
12. Madon, R. J., and Taylor, W. F., *J. Catal.* **69,** 32 (1981).
13. Schulz, H., Beck, K., and Erich, E., *Stud. Surf. Sci. Catal.* **36,** 457 (1988).
14. Madon, R. J., and Taylor, W. F., *Adv. Chem. Ser.* **178,** 93 (1979).
15. Flory, P. J., *J. Am. Chem. Soc.* **58,** 1877 (1936).
16. Schulz, H., Rosch, S., and Gokcebay, H., *in* "Proceedings, Symposium on Coal: Phoenix of the 80's, 64th Annual CIC Conference, Halifax, Canada" (Al Taweel, A. M., Ed.), 486, 1982.
17. Boudart, M., "Kinetics of Chemical Processes," Prentice-Hall, Englewood Cliffs, NJ, 1968.
18. Konig, L., and Gaube, J., *Chem. Ing. Tech.* **55,** 14 (1983).
19. Huff, G. A., and Satterfield, C. N., *J. Catal.* **85,** 370 (1984).
20. Egiebor, N. O., and Cooper, W. C., *Appl. Catal.* **14,** 323 (1985).
21. Rice, N. M., and Wojciechowski, B. J., *Can. J. Chem. Eng.* **65,** 102 (1987).
22. Tau, L-M., Dabbagh, H., Bao, S., and Davis, B. H., *Catal. Lett.* **7,** 127 (1990).